Proceedings of the Korean Nuclear Society Spring Meeting
Kwangju, Korea, May 2002

Thermal Hydraulic Analysis of Thorium Fuel Assemblies Loaded with Annular Seed Pins

Kyu Hyun Han, Soon Heung Chang

Korea Advanced Institute of Science and Technology
373-1, Guseong-dong, Yuseong-gu, Daejeon, 305-701, Republic of Korea

Abstract

Thermal hydraulic characteristics of thorium-based fuel assemblies loaded with annular seed pins have been analyzed using MATRA_A combined with MATRA, and compared with those of the existing thorium-based assemblies. MATRA and MATRA_A showed good agreements for the pressure drops at the internal subchannels. The pressure drop generally increased in the cases of the assemblies loaded with annular seed pins due to the larger wetted perimeter, but an exception existed. In the inner subchannels of the seed pins, mass fluxes were high due to the grid form losses in the outer subchannels. About 43% of the heat generated from the seed pin flowed into the inner subchannel and the rest into the outer subchannel, which implies the inner to outer wall heat flux ratio was approximately 1.2. The maximum temperatures of the annular seed pins were slightly above 500°C. The MDNBRs of the assemblies loaded with annular seed pins were higher than those of the existing assemblies. Due to the fact that interchannel mixing cannot occur in the inner subchannels, temperatures and enthalpies were higher in the inner subchannels.

Introduction

The thorium-based fuel cycle has attracted attention because it promises a number of benefits relative to the conventional uranium-based cycle for commercial reactors. Benefits include the enhanced proliferation resistance characteristics of the spent fuel which originate in the reduced plutonium generation and the enhanced in-core fissile material generation capability, that is, the higher thermal absorption cross section for Th^{232} than for U^{238}, which reduces the need of fuel ore and the enrichment per unit of energy generation.

There are two alternative designs of thorium fuel assemblies. One of them is the Seed-Blanket Unit (SBU) [6] which is equal in outer dimensions to the conventional pressurized water reactor (PWR) fuel assembly. The SBU consists of two separate regions. The inner region of the unit called the seed supplies neutrons to the outer region called the blanket which generates fissile materials. The seed region requires smaller fuel pin diameter and/or fuel material with higher conductivity than the blanket region. This design is known as the Radkowsky Thorium Fuel (RTF) concept. The other design is the Whole Assembly as Seed or Blanket (WASB) [1] where each type of fuel occupies a whole PWR assembly. These two types of assemblies are arranged in a checkerboard distribution.

The main drawback of the two designs from a thermal hydraulic perspective is the high power imbalance between the seed and the blanket region. To remedy this, the heat removal in the seed region should be enhanced. Recently, the annular fuel pin was proposed by NERI [3] to be implemented in current PWR cores to achieve a significant increase of core power density while improving safety margins. It can be applied to the thorium fuel assemblies for the enhanced heat removal in the seed region. Figure 1 shows an annular fuel pin. Subchannel codes such as MATRA [2] capable of modeling the entire core are necessary to capture the benefits of mixing effects which improve DNBR in the hot channel. MATRA (Multichannel Analyzer for steady states and Transients in Rod Arrays; KAERI) is the thermal hydraulic analysis code developed by KAERI (Korea Atomic Energy Research Institute) based on the COBRA-IV-I. MATRA calculates the local thermal hydraulic conditions, such as flow, enthalpy, pressure, and void fraction in each flow channel and the MDNBR (Minimum Departure from Nucleate Boiling Ratio) in the hot subchannel using some proper CHF (Critical Heat Flux) correlations. However, the current version of MATRA does not have the capability to model both internally and externally cooled annular fuel pins. Therefore, to analyze the thermal hydraulics of thorium fuel assemblies loaded with annular seed pins, a subchannel code with capabilities to calculate the coolant flow distribution between internal and external channels and heat flow split into individual channels is needed.

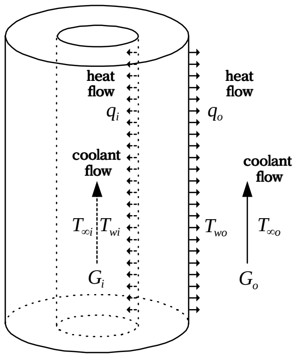

Figure 1 Annular fuel pin

Nomenclature

Δp	: pressure drop	Pa
ρ	: density	kg/m^3
g	: gravitational acceleration	m/s^2
z	: elevation	m
T	: temperature	^oC
α	: void fraction	
G	: mass flux	$kg/m^2\ s$
x	: quality	
D_e	: equivalent diameter	m
q''	: heat flux	kW/m^2
h	: heat transfer coefficient	$kW/m^2\ s$
k	: thermal conductivity	kW/m K
L	: length	m
P	: pitch	m
D	: diameter	m

Subscripts

SCB : subcooled boiling
BB : bulk boiling
grav : gravitation
acc : acceleration
fric : friction
m : mass
f : fluid
g : gas
iso : isothermal
sat : saturation
w : wall
i : inner
o : outer

Development of An Attachable Program

A search for a subchannel code with capabilities to model innovative internally and externally cooled annular fuel pins has been in vain so far. Thus, this study is mainly focused on providing a method to analyze fuel assemblies loaded with annular fuel pins laying special emphasis on coolant and heat flow split into internal and external channels, combining it with MATRA, and comparing thorium fuel assemblies loaded with annular seed pins of preliminary designs with those loaded with cylindrical ones from a thermal hydraulic perspective.

Coolant Flow Split

The proposed annular fuel pin introduces a new variable that needs to be considered in the calculation – partial coolant flow penetrating the annular pin in the axial direction. The coolant flow must be distributed in the manner of equalizing pressure drops in all the subchannels. However, MATRA offers channel inlet flows split option for equal pressure gradient across the first axial node only. Therefore, the coolant flow distribution must be adjusted by an adequate pressure drop model. The calculations of the pressure drop in a heated channel allowing for nonequilibrium conditions such as nonequal velocity and nonsaturated phases are considered in this study. Essentially, four flow regions may exist over the entire length of the subchannel [4]. They are regions of the single phase liquid, subcooled boiling, bulk boiling and single phase vapor. However, only two of them, that is, regions of the subcooled and bulk boiling, are considered here for simplicity, as shown in Figure 2. The existence of these flow regions depends on the heat flux and the inlet conditions. The total pressure drop can be obtained as the summation of the pressure drops over each axial region:

$$\Delta p_{total} = \Delta p_{SCB} + \Delta p_{BB} \tag{1}$$

where:

$\Delta p_{SCB} =$ pressure drop in the subcooled boiling region

$\Delta p_{BB} =$ pressure drop in the bulk boiling region

Three components of pressure drop, that is, elevation, acceleration and friction, over each region are considered here. The total pressure drop without any form pressure losses is given by:

$$\Delta p_{tot} = \sum_{i=0}^{1}\left[\int_{z_i}^{z_{i+1}} \rho g dz + \frac{G_m^2}{\rho_f}(r_2)_{z_i}^{z_{i+1}} + \int_{z_i}^{z_{i+1}} \frac{\phi_{\ell o}^2 f_{\ell o} G_m^2}{2\rho_f D_e} dz\right] \tag{2}$$

where each numerical index corresponds to each transition point, including inlet and outlet.

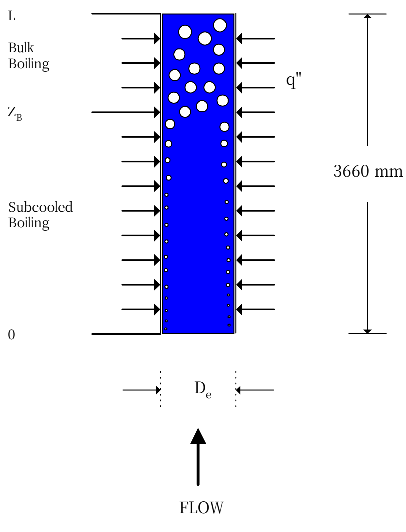

Figure 2 Subchannel flow regions

Heat Flow Split

Another new variable to be considered is the partial heat flow directed to the inner channel of the annular pin. All current PWR cores employ fuel pins cooled at their external surface by an open flow, hence all the energy generated within the pin is transferred to the flow stream along the fuel pin array. However, in the annular fuel pin with an internal cooling hole, only part of the heat rate generated in a fuel pellet will be transferred to the external coolant in the open fuel pin array and the remaining part will be transferred to the internal coolant flowing through the hole. The current version of MATRA is not capable of modeling fuels other than cylindrical and plate fuels. Therefore, the heat flow split must be given by an adequate heat transfer model. For the heat transfer coefficient, in the particular case of water, Weisman gave:

$$(Nu_{\infty})_{c.t.} = 0.023\,\mathrm{Re}^{0.8}\,\mathrm{Pr}^{0.333} \tag{3}$$

$$\psi = 1.826P/D - 1.0430 \tag{4}$$

On the other hand, the wall temperatures of the fuel pins are given by the heat equation:

$$\frac{1}{r}\frac{\partial}{\partial r}\left(kr\frac{\partial T}{\partial r}\right)+\frac{1}{r^2}\frac{\partial}{\partial \phi}\left(k\frac{\partial T}{\partial \phi}\right)+\frac{\partial}{\partial z}\left(k\frac{\partial T}{\partial z}\right)+\dot{q}=\rho c_p\frac{\partial T}{\partial t} \tag{5}$$

From the equality of power fraction:

$$q_i : q_o = r_m^2 - r_i^2 : r_o^2 - r_m^2 \tag{6}$$

where r_m satisfies the equation:

$$\left.\frac{dT}{dr}\right|_{r=r_m} = 0, \tag{7}$$

the power directed to the internal and external channels can be calculated by the relations, respectively:

$$q_i = h_i A_i (T_{wi} - T_{\infty i}) \tag{8}$$

$$q_o = h_o A_o (T_{wo} - T_{\infty o}) \tag{9}$$

An Attachable Program

Using the models described above, a program named MATRA_A which can be attached to MATRA and calculate coolant and heat flow split in the annular fuel pin has been developed. To begin with, additional isolated inner subchannels of the annular seed pins are defined in the input data. Then MATRA is executed using the input. When MATRA finishes the calculation, coolant temperature, mass flux, density, quality and void fraction of each subchannel are collected. From the collected data, heat transfer coefficients of the coolant and temperatures of inner and outer surfaces of the seed pins are calculated. Finally, pressure drop in each inner subchannel and heat flow directed to the inner and outer subchannels are calculated from the previous result. The next step is to check if the previously assumed mass flow distribution and power fraction are within the allowable margin of error. If they are, the calculation stops, but if they are not, different mass flow distribution and power fraction are assumed and MATRA is executed again. This loop is repeated until the mass flow distribution and power fraction are within the error tolerance. The flow chart of MATRA_A is given in Figure 3.

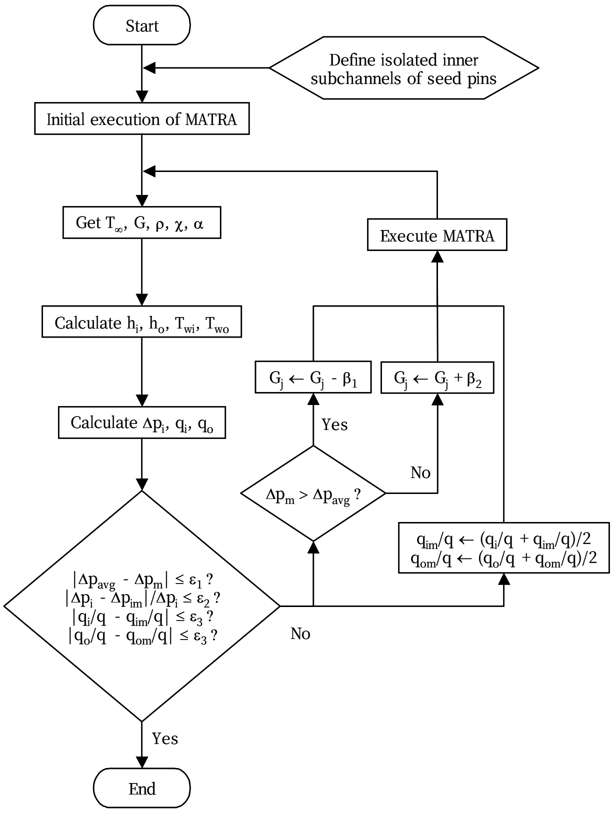

Figure 3 Flow chart of MATRA_A

Thorium Fuel Assemblies Loaded with Annular Seed Pins

The preliminary designs of annular seed pins for thorium fuel assemblies have been done based on the dimensions of the existing thorium fuel assemblies. The thicknesses of the annular fuel pellet and the gas gap are 0.96 mm and 0.085 mm, respectively, which are the same as those of the WASB-B seed pin. The cladding thickness is 0.4 mm for all three kinds of the seed pin as before. The three thorium fuel assemblies loaded with annular seed pins are named SBU_A, WASB-A_A and WASB-B_A respectively, where the '_A' implies 'annulus'. Also, the seed pins of the SBU_A and the WASB-A_A are identical as before. Table 1 summarizes the most relevant design parameters of the three alternatives. The core radial and axial power distributions were taken from the SBU MOC results [1] in order to analyze and compare the different alternative designs as before. In the case of the SBU_A, one whole unit is analyzed, however, in the case of the WASB_A, the selected modeling region, as shown in Figure 4, was taken as the symmetric volume composed of one quarter each of two seed assemblies and one quarter each of two blanket assemblies. The relative pin power distributions for the SBU_A, WASB-A_A and WASB-B_A were available at an assembly level. Subchannels and rods were also defined in a similar way as was done for the existing thorium fuel assemblies. An example for WASB-B_A is shown in Figure 5.

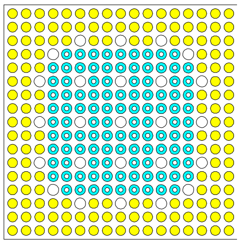

(a) SBU_A

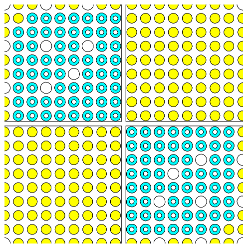

(b) WASB-A_A

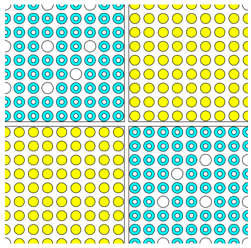

(c) WASB-B_A

Figure 4 Selected modeling regions

Table 1 Design parameters of three alternative assemblies loaded with annular seed pins

Parameter	SBU_A		WASB-A_A		WASB-B_A	
	Seed	Blanket	Seed	Blanket	Seed	Blanket
Fuel Assembly Width [cm]	21.4		21.4	21.4	21.4	21.4
Fuel Assembly Gap [cm]	0.11		0.11	0.11	0.11	0.11
Fuel Material Composition	U/Zr metal alloy (45%/55% in weight) U 20% enriched	$(U+Th)O_2$ (10% UO_2/90% ThO_2 in weight) U 15% enriched	U/Zr metal alloy (45.3% U, 54.7% Zr) U 20% enriched	$(U+Th)O_2$ (10% UO_2/90% ThO_2 in weight) U 15% enriched	UO_2 U 20% enriched	$(U+Th)O_2$ (10% UO_2/90% ThO_2 in weight) U 15% enriched
Number of Fuel Rods	108	156	236 seed rods 28 adjusted rods 25 control/guide rods	288 blanket rods 1 guide tube	264 seed rods 25 control/guide rods	288 blanket rods 1 guide tube
Fuel Pellet Radius [cm] inner-outer	0.3905-0.4865	0.0-0.4095	0.3905-0.4865	0.0-0.4095	0.3905-0.4865	0.0-0.4095
Fuel-Clad Gap [cm]	0.0085	0.0085	0.0085	0.0085	0.0085	0.0085
Cladding Material Thickness [cm]	0.04	0.057	0.04	0.057	0.04	0.057
Rod Diameter [cm]	1.070	0.950	1.070	0.950	1.070	0.950
Fuel Cell Pitch [cm]	1.26	1.26	1.26	1.26	1.26	1.26

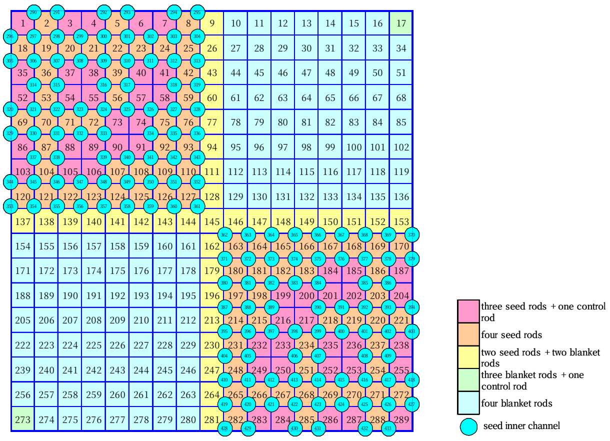

(a) Subchannel identification

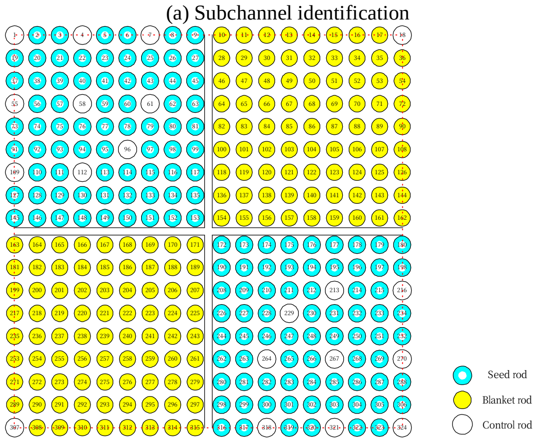

(b) Rod identification

Figure 5 WASB-B_A subchannel and rod identification

Thermal Hydraulic Analysis

Assuming that the operating parameters of the thorium-based reactors loaded with annular seed pins are the same as those of a typical Westinghouse 4-loop PWR, as shown in Table 2, thermal hydraulic analyses have been performed using MATRA and MATRA_A.

Table 2 Operating parameters of a typical Westinghouse 4-loop PWR

Parameter	Value
Core Heat Output [MWth]	3400
System Pressure [MPa]	15.5
Effective Flow Rate [Mg/s]	17.7
Active Fuel Height [cm]	366
Number of Assemblies	193
Inlet Coolant Temperature [°C]	289

The average pressure drops of the six alternative designs are given in Figure 6. The calculations for the existing assemblies are done using MATRA. The assemblies loaded with annular seed pins cause higher pressure drop than the existing ones because they have larger wetted perimeter due to the additional cladding volume. However, in the case of WASB-B_A, pressure drop decreased compared with WASB-B, which might be explained by 'offset effect' by high MDNBR. Figure 7 shows hottest cell pressure drop of the WASB-A_A. It is clear from the Figure that relatively higher coolant temperature in the inner subchannel brings about pressure drop which is equal to the outer subchannel pressure drop mainly caused by the grid spacers.

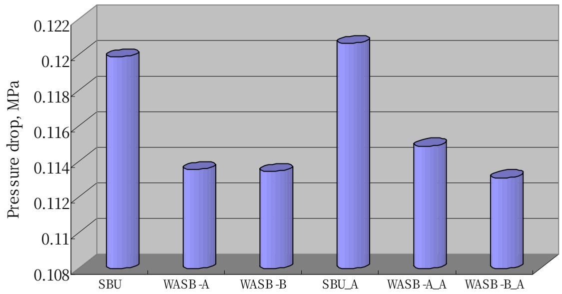

Figure 6 Comparison of average pressure drops

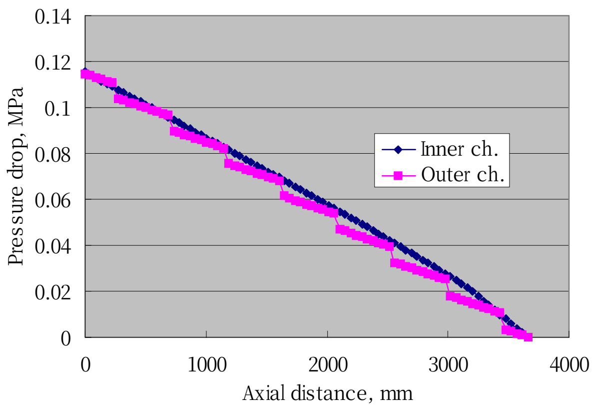

Figure 7 Hottest cell axial pressure drop profiles for the WASB-A_A

(Inner subchannel ID is 349.)

In the cases of the assemblies loaded with annular seed pins, as the outer diameter of the seed pin is larger than that of the blanket pin, mass fluxes in the outer subchannels of the seed pins are low, as shown in Figures 8, 9 and 10 for SBU_A, WASB-A_A and WASB-B_A respectively. In the inner subchannels of the seed pins, mass fluxes are high due to the grid form losses in the outer subchannels. Figure 11 gives power fractions of the annular seed pins. About 43% of the heat generated from the seed pin flows into the inner subchannel and the rest into the outer subchannel, which implies the inner to outer wall heat flux ratio is approximately 1.2. Figure 12 shows radial temperature profiles at the hottest axial positions in the hottest annular seed pins. For the fuel-clad gap, a constant conductance of 1000 Btu/hr-ft^2-°F, which is typical for PWR fuel, was assumed. The maximum temperatures of the seed pins are approximately 501°C, 513°C and 515°C for the SBU_A, WASB-A_A and WASB-B_A respectively. The MDNBR profiles are given in Figure 13, which clearly identifies higher thermal margins of the assemblies loaded with annular seed pins compared with the existing ones. As significant different power levels can be found in the seed region compared with the blanket region, the analysis must be done at the hottest spot in the fuel. In this case, the hottest subchannel shows the higher temperature found in the fuel.

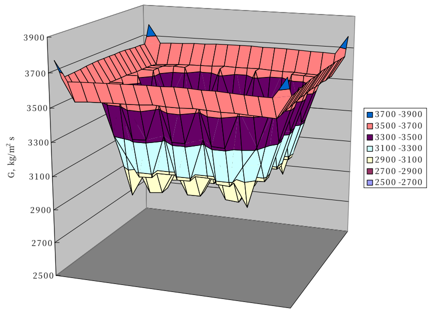

(a) Outer subchannels

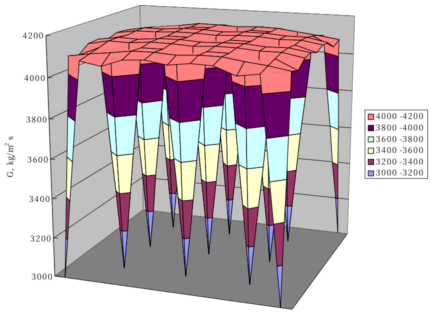

(b) Inner subchannels

Figure 8 Exit mass flux distributions of the SBU_A

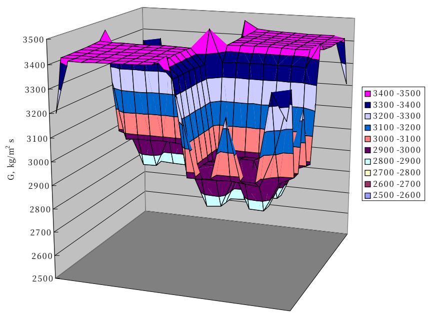

(a) Outer subchannels

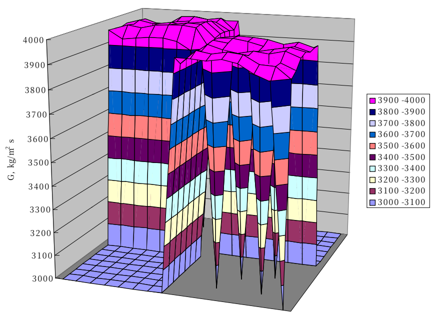

(b) Inner subchannels

Figure 9 Exit mass flux distributions of the WASB-A_A

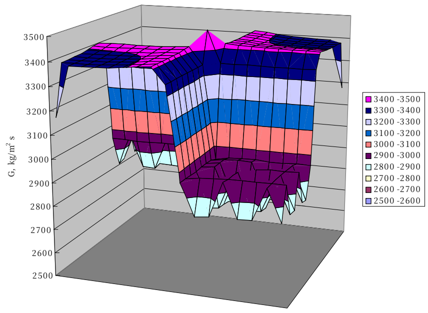

(a) Outer subchannels

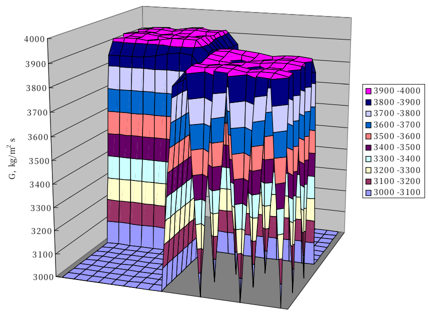

(b) Inner subchannels

Figure 10 Exit mass flux distributions of the WASB-B_A

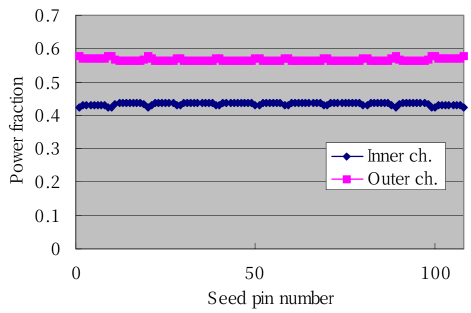

(a) SBU_A

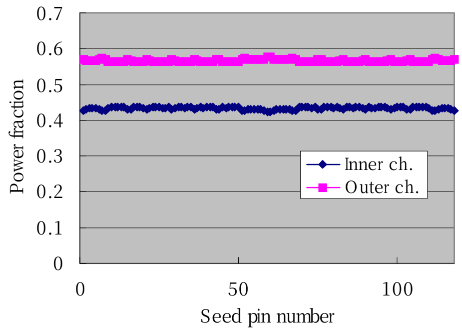

(b) WASB-A_A

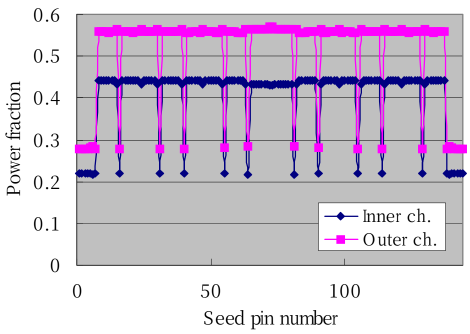

(c) WASB-B_A

Figure 11 Power fractions of the annular seed pins

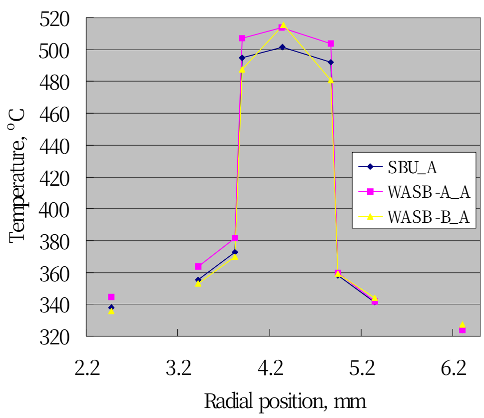

Figure 12 Radial temperature profiles at the hottest axial positions in the hottest annular seed pins

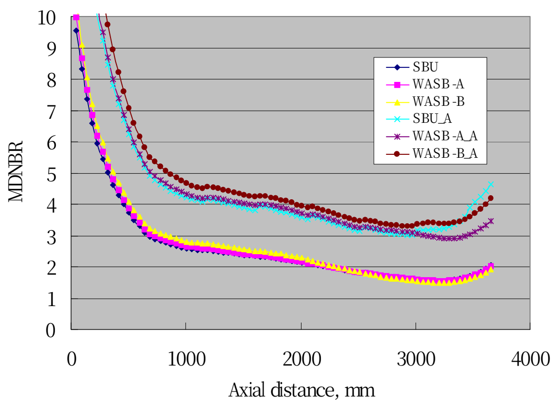

Figure 13 MDNBR profiles

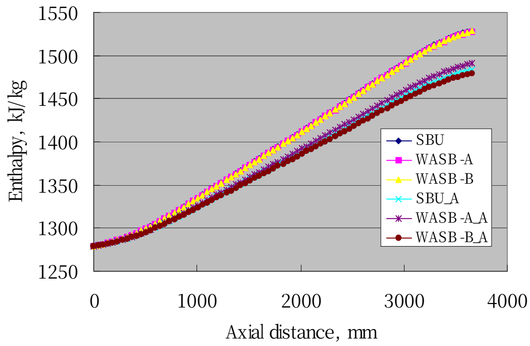

Figure 14 Average enthalpy profiles

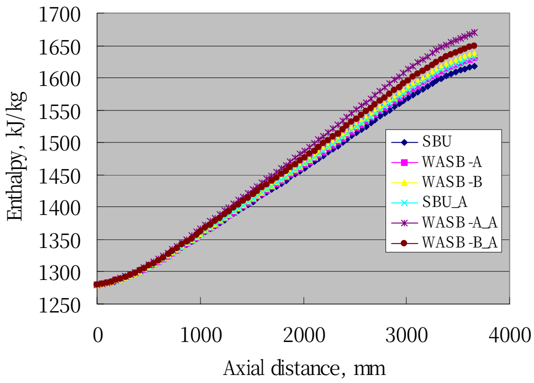

Figure 15 Hottest subchannel enthalpy profiles

The average enthalpy profiles given in Figure 14 together with the hottest subchannel profiles given in Figure 15 reveal that heat transfer to the coolant is heavily biased toward some hot subchannels in the cases of the assemblies loaded with annular seed pins. Figures 16, 17 and 18 give the exit enthalpy profiles of the SBU_A, WASB-A_A and WASB-B_A respectively. They provide a good sense of the impact of different power levels between the seed region and the blanket region, and also show the hot locations within the assemblies. The enthalpies in the inner subchannels are higher than those in the outer subchannels owing to the fact that interchannel mixing cannot occur in the inner subchannels. It is desirable to achieve approximately the same coolant enthalpy rise in both of the outer and inner subchannels. On the whole, the assemblies loaded with annular seed pins show better thermal hydraulic performances than the existing assemblies.

Conclusions

The most important challenge for all of the analyzed designs loaded with annular seed pins was to deal with the coolant and heat flow split into internal and external channels. The power fraction tolerance was set at 0.1%, the tolerance of the pressure drops among subchannels 0.005 MPa, and the tolerance between MATRA's and MATRA_A's pressure drop results at internal subchannels 5%. The calculation results are summarized as follows:

(1) The pressure drop generally increases in the cases of the assemblies loaded with annular seed pins due to the larger wetted perimeter, but an exception exists.

(2) In the inner subchannels of the seed pins, mass fluxes are high due to the grid form losses in the outer subchannels.

(3) About 43% of the heat generated from the seed pin flows into the inner subchannel and the rest into the outer subchannel, which implies the inner to outer wall heat flux ratio is approximately 1.2.

(4) The maximum temperatures of the annular seed pins are slightly above 500°C.

(5) The MDNBRs of the assemblies loaded with annular seed pins are higher than those of the existing assemblies.

(6) Due to the fact that interchannel mixing cannot occur in the inner subchannels, enthalpies are higher in the inner subchannels.

References

[1] M. Busse and M. S. Kazimi, Thermal and economic analysis of thorium-based seed-blanket fuel cycles for nuclear power plants, MIT-NFC-TR-025, 2000.
[2] Y. J. Yoo and D. H. Hwang, Development of a subchannel analysis code MATRA, KAERI/TR-1033/98, 1998.
[3] M. S. Kazimi et al., High performance fuel design for next generation PWRs, NERI proposal, 2001.
[4] N. E. Todreas and M. S. Kazimi, Nuclear systems I – thermal hydraulic fundamentals, MIT, 442-457, 537-546, 605-614, 1990.
[5] A. G. Morozov et al., A thorium-based fuel cycle for VVERs and PWRs, Nucl. Eng. Int'l, 13-14, 1999.
[6] A. Radkowsky, Using thorium in a commercial nuclear fuel cycle: how to do it, Nucl. Eng. Int'l, 14-16, 1999.
[7] A. Galperin et al., A pressurized water reactor plutonium incinerator based on thorium fuel and seed-blanket assembly geometry, Nuclear Technology, Vol.132, 214-226, 2000.
[8] A. Radkowsky and A. Galperin, The nonproliferative light water thorium reactor: a new approach to light water reactor core technology, Nuclear Technology, Vol. 124, 215-222, 1998.
[9] J. R. Lamarsh, Introduction to nuclear engineering, 353-396, 1983.
[10] F. P. Incropera and D. P. DeWitt, Fundamentals of heat and mass transfer, 52-60, 1996.